Activated Carbon Derived from Pyrolyzed Pinewood Char using Elevated Temperature, KOH, H_3PO_4, and H_2O_2

Yan Luo, Jason Street,* Philip Steele, Edward Entsminger, and Vamshi Guda

Activated carbon was prepared from pyrolyzed pinewood char using KOH, H_3PO_4, H_2O_2, and heat-only treatments. Activated carbon prepared by the heat-only treatment had a total surface area of 233.2 m^2/g, a total pore volume of 0.138 cm^3/g, a microporous surface area of 129.9 m^2/g, and a microporous volume of 0.07 cm^3/g. The most significant improvement of pore properties for the chemically treated pinewood char was obtained by the KOH treatment, which produced a total surface area of 1124.4 m^2/g, a total pore volume of 0.723 cm^3/g, a microporous surface area of 923.6 m^2/g, and a microporous volume of 0.485 cm^3/g. After the H_3PO_4 treatment, pinewood char had a total surface area of 455.5 m^2/g, a total pore volume of 0.251 cm^3/g, a microporous surface area of 393.3 m^2/g, and a microporous volume of 0.211 cm^3/g. The least significant improvement was obtained from the H_2O_2 treatment, which produced a total surface area of 363.0 m^2/g, a total pore volume of 0.202 cm^3/g, a microporous surface area of 271.5 m^2/g, and a microporous volume of 0.141 cm^3/g. Transmission electron microscopy (TEM), thermogravimetric analysis (TGA), and Fourier transform infrared spectroscopy (FTIR) were performed to compare separate treatment stabilities and functional group properties.

Keywords: Activated carbon; Pyrolyzed pinewood char; KOH; H_2O_2; H_3PO_4

*Contact information: Department of Sustainable Bioproducts, Mississippi State University, PO Box 9820, Mississippi State, MS 39762-9820 USA; *Corresponding author: jason.street@msstate.edu*

INTRODUCTION

Activated carbon is a carbon-based material with high surface area, exceptional absorption/adsorption ability, high chemical resistance, and high mechanical strength. Commercial activated carbon possesses a surface area ranging from 500 to 2000 m^2/g (Williams and Reed 2006), and some super-activated carbon products have surface areas above 2000 m^2/g (Khummongkol *et al.* 1992). According to the International Union of Pure and Applied Chemistry (Sing 1985), there are three types of pores relevant to porosity: micropores (< 2 nm), mesopores (2 to 50 nm), and macropores (> 50 nm). Micropores can be divided into ultramicropores (< 0.7 nm) and supermicropores (0.7 to 2 nm). The pore size in the activated carbon determines its application areas because they have an effect on the porosity, the total surface area that is available for adsorption, and the size of molecules that can diffuse into the solid. Microporosity relates to the activated carbon adsorption capacity, while mesoporosity provides the channels for transportation of the adsorbate and is positively correlated with high levels of adsorbate. Macroporosity makes no contribution to the adsorption capacity, but it may assist with transport of the adsorbate into the interior of the particle (Williams and Reed 2006).

Activated carbon is used for the separation and purification of various chemicals (Amaya *et al.* 2007). The use of activated carbon is expected to grow in the U.S. at approximately 3% annually, which is mostly driven by further environmental applications. Activated carbon is mainly produced from petroleum coke and coal. However, future reductions in greenhouse gases will eventually require the decreased use of fossil fuels and their byproducts. There is a search underway for sustainable and environmentally friendly resources to produce activated carbon from biomass resources. Potential carbon-rich biomass precursors for activated carbon production are diverse and include wood, numerous straw varieties, coconut shell, walnut shell, apricot pit, bamboo, and various grasses (Cunliffe and Williams 1999). According to the International Biochar Initiative Organization, by the year 2050, about 80% of all crop and forestry residues will be converted to biochar and energy (Kołodyńska *et al.* 2012). Specifically, the reuse of biomass waste can bring substantial benefits to regional economies. Therefore, the development of an integrated process to make full use of biomass to provide both liquid fuels and solid activated carbon would be beneficial.

In the U.S., wood comprises the highest volume component of biomass resources. The pyrolysis of pinewood results in the highest bio-oil yield, at 62 wt.%, compared with other wood species (Oasmaa *et al.* 2009) because of its lower mineral content and higher lignin content. Pyrolyzed char without any treatment is used as an amendment or used as fuel *via* direct combustion (Woolf *et al.* 2010). Moreover, pyrolyzed char has the potential for conversion to activated carbon with high surface area with controlled porosity for specific purposes. This would allow activated carbon prepared from pyrolyzed char to compete with activated carbon now produced from coal and petroleum.

Activated carbon production, regardless of the carbon source, can be divided into two steps, which are carbonization and activation. Carbonization is conducted at high temperatures ranging from 400 to 1200 °C with limited oxygen to pyrolyze the raw feedstock into a multiple-pore carbon material. Following carbonization, the activation step is continued by chemical, physical, or chemical-physical methods to form a well-developed pore structure. Possible chemical activators include K_2CO_3, KOH, NaOH, H_3PO_4, NH_4Cl, HCl, H_2SO_4, $ZnCl_2$, $FeCl_3$, and $MgCl_2$. The activation process requires four steps to improve the surface area of the carbon structure, which are the further development of existing but previously inaccessible pores, the creation of new pores by selective activation, widening of existing pores, and the merging of existing pores due to pore wall breakage (Rodríguez-Reinoso and Molina-Sabio 1992).

The activation conditions that influence activated carbon properties include carbonization temperature, carbonization time, activation time, activation temperature, activator types, and the amount of activator applied. Chemical activation has three main merits. It is performed in a single step. Thus, carbonization and activation are completed in the same step, and the process is conducted at a relatively low temperature compared with physical methods (Tay *et al.* 2009). In addition, the chemical activation time is considerably shorter, and functional groups are formed during the chemical activation process. However, chemical activators have drawbacks, which include potential environmental pollution and acid or alkali corrosion of the processing equipment. Also, some chemical components remain on the activated carbon and limit the range of its applications.

Activated carbon with differing pore properties have been prepared from various biomass feedstocks using KOH and H_3PO_4 treatments, but not much research has been carried out using H_2O_2 as a treatment. Zabaniotou *et al.* (2008) prepared activated carbon

from the pyrolyzed char of olive kernels using a KOH treatment. The activated carbon created from these olive kernels possessed a total surface area of 2159 m^2/g and contained 78% micropores.

Macias-Garcia *et al.* (2007) applied various concentrations of water to H_3PO_4 (1:1, 1:2, and 1:3) to activate chestnut wood at temperatures ranging from 300 to 600 °C in a single process. A more heterogeneous micropore structure was produced when the highest acid concentration was applied at 300 °C or when a lower acid concentration was applied at 600 °C. The microporous pore size distribution was similar at 400 °C and 500 °C regardless of the H_3PO_4 concentration. The largest degree of surface area development and microporosity were obtained at 500 °C with a surface area of 783 m^2/g and a total pore volume of 0.431 cm^3/g.

Duman *et al.* (2009) produced activated carbon from a pine cone feedstock by separately applying H_3PO_4 and $ZnCl_2$ activators. The surface area and micropore volume of activated carbon from the $ZnCl_2$ activator were somewhat higher than that produced by the H_3PO_4 activation. When the $ZnCl_2$ impregnation ratios were between 50 and 200 wt.%, the activated carbon had a surface area between 819 and 1816 m^2/g, while the activated carbon prepared with H_3PO_4 had a surface area ranging 1148 and 1597 m^2/g.

Rios *et al.* (2009) applied H_3PO_4 to a coconut shell feedstock to prepare activated carbon. The impregnation process was performed at 85 °C for 2 h with a H_3PO_4 solution at increasing concentrations of 29, 36, 44, and 53 wt.%. After impregnation, the specimens were carbonized in an ambient air atmosphere at 450 °C with a heating rate of 1 °C/min for 2 h. The H_3PO_4 concentration of 36% produced the optimum quality of activated carbon. Moreover, the total surface area and microporosity increased greatly when nitrogen was added as a blanket gas during the coconut carbonization process compared to results obtained without nitrogen. The best specimen had a surface area of 844 m^2/g and a total pore volume of 0.55 cm^3/g. Elevated temperature studies (750 ^oC) using pine biochar created at 450 ^oC and the particular treatments used in this work (especially with H_2O_2) need further research. The objective of this study was to prepare activated carbon with a high surface area from pyrolyzed pinewood char directly using KOH, H_2O_2, and H_3PO_4, and a heat-only treatment as a control. The physical properties of each activated carbon prepared by the four separate treatments were compared by various analytical methods.

EXPERIMENTAL

Loblolly pinewood (*Pinus taeda*) was purchased at a local lumberyard near Mississippi State University. Potassium hydroxide (KOH, Pellets/Certified ACS), phosphoric acid (H_3PO_4, ACS reagent, 85+% solution in water), hydrogen peroxide (H_2O_2, 30 wt.%, Certified ACS), filter paper, and a pH meter were purchased from Fisher Scientific (Hampton, NH, USA). Helium (ultra-high purity), nitrogen (ultra-high purity), and liquid nitrogen were purchased from NexAir (Columbus, MS, USA). Distilled water was prepared in the laboratory. The chemicals and gases were used directly without any further purification.

Treatment of the Pyrolyzed Pinewood Char

Pinewood lumber was comminuted to particles of 1 to 3 mm and then dried to less than 5 wt.% moisture content. Pyrolysis was performed at 450 °C with a nitrogen blanket gas in an auger reactor, using process conditions described in previous studies (Ingram *et*

al. 2007; Luo *et al.* 2016a,b,c), a feed rate of 1 kg/h, and an auger speed of 13 rpm. During pyrolysis, the volatilized char produced was automatically fed into an airtight container to prevent combustion of the hot char and then cooled to room temperature before removing it from the system. The pyrolyzed char was sieved to a uniform size ranging from 60 to 80 mesh. The char was dried at 110 °C in a vacuum oven for 24 h to remove moisture and gas adsorbed onto the surface. Treatment of pyrolyzed char was performed by mixing dried pyrolyzed char with a concentrated solution of activators in a 1:1 weight ratio of activator to pyrolyzed char (5 g KOH, 5 g H_3PO_4, 5 g H_2O_2 dissolved in 20 g H_2O and then mixed with 5 g char, respectively). The mixture was kept in a beaker at ambient room temperature for 24 h. The treated pyrolyzed char was then dried a second time at 110 °C in a vacuum oven for 24 h. The dried mixture, consisting of the pyrolyzed char and the activator, was saved for thermo-chemical activation.

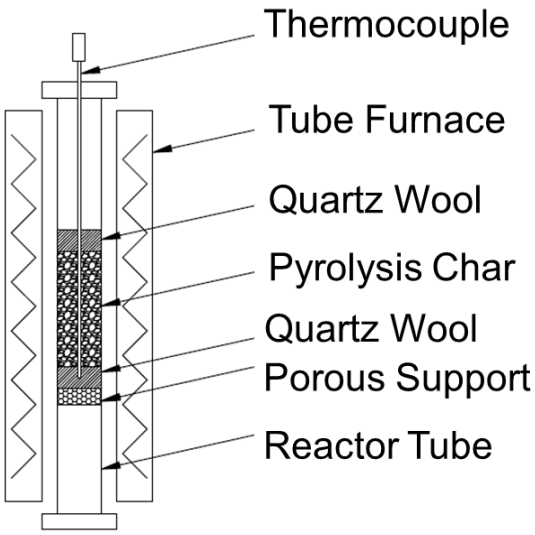

Fig. 1. Schematic diagram of the micro-reactor tube used for thermochemical activation

Thermochemical Activation of the Pyrolyzed Pinewood Char

A fixed-bed micro-reactor (Micrometrics Instrument Corp., Norcross, GA, USA) was used to thermochemically treat the pyrolyzed char. This thermochemical treatment carbonized and activated the pyrolyzed char simultaneously. The micro-reactor vessel is shown in Fig. 1. The micro-reactor was comprised of a 60 cm long stainless steel vessel with a 12 mm diameter. The micro-reactor was electronically heated by a tubular ceramic furnace, which was equipped with a photoionization detector temperature control with a type K thermocouple placed at the center. In each experiment, a 5 mm thick quartz wool bed was loaded into the tube on the top of a porous support and 0.3 g of the pyrolyzed pinewood char was weighed and placed in the reactor tube. A quartz wool bed 5 mm thick was placed above the pyrolyzed char. At the beginning of the experiment, helium was run through the micro-reactor for 0.5 h to ensure inert conditions in the reactor. The furnace was then heated to a final temperature of 750 °C at a heating rate of 5 °C/min.

When the micro-reactor temperature reached the 750 °C set point, the reactions were maintained for 1 h at a helium flow rate of 100 mL/min. Following activation, the sample in the reactor was cooled to ambient room temperature under a helium flow rate of

100 mL/min. The products were removed from the micro-reactor and weighed. The product yield was calculated by Eq. 1,

$$Yield\ (wt\%) = (m_1 - m_2) / m_1 \quad (1)$$

where *Yield (wt%)* is the activated carbon yield in terms of weight percentage, m_1 is the mass of pyrolyzed char placed into the micro-reactor before activation (g), and m_2 is the mass of the products after the activation (g).

The products were subsequently washed with hot distilled water several times in a beaker until the pH of the washed solution was 7 (Zabaniotou *et al*. 2008). The washed samples were dried at 110 °C for 24 h in a vacuum oven for moisture removal and then sieved to a uniform size ranging from 60 to 80 mesh for the Brunauer-Emmett-Teller (BET) method, thermogravimetric analysis (TGA), transmission electron microscopy (TEM) analysis, and Fourier transform infrared spectroscopy (FTIR) analysis.

Adsorption-Desorption Isotherm Characterization

The porous texture parameters of the activated carbon were determined by adsorption-desorption isotherms of nitrogen measured at -196 °C with an AutosorbiQ gas sorption analyzer (Quantachrome, Boynton Beach, FL, USA). Prior to gas adsorption measurements, specimens were degassed at 300 °C under a vacuum for 6 h at a heating rate of 2 °C/min. The apparent surface area of the activated carbon was calculated by the BET method (Gregg and Sing 1982). The microporous surface area was determined by the t-plot method. The total pore volume was determined by converting nitrogen gas adsorbed at a relative pressure of 0.99 to the volume of liquid adsorbate (nitrogen).

Transmission Electron Microscopy (TEM) Analysis

A high-resolution transmission electron microscope (JEOL JEM-100CX II, JEOL USA Inc., Peabody, MA, USA), operated at 200 kV and 112 µA, was used to examine the activated carbon porosity. A small amount of each specimen was ground to powder, and an appropriate volume of ethanol at a concentration of 100% was added to disperse the powder. The sample was sonicated for 30 min and allowed to stand for 24 h. One drop of this suspension was placed on a Formvar 300 mesh copper grid and allowed to air dry before TEM characterization was performed.

Thermogravimetric Analysis (TGA)

TGA was performed to determine thermal degradation of the activated char. Specimens were analyzed in an Al_2O_3 crucible on a Mettler Toledo TGA/STD 851 analyzer (Thermo Scientific, Waltham, MA, USA). Specimens were dried at 100 °C for 24 h in a vacuum oven. Subsequently, each specimen, weighing 8 to 10 mg, was heated from ambient room temperature to a final temperature of 1000 °C at a heating rate of 10 °C/min using a nitrogen flow rate of 100 mL/min.

Fourier Transform Infrared Spectroscopy (FTIR)

FTIR analysis was performed using a Thermo Scientific Nicolet iS50 FTIR spectrometer (Thermo Scientific, Waltham, MA, USA). Specimens were dried at 100 °C for 24 h in a vacuum oven, and then placed in the sample cell for analysis. For each specimen, a total of 64 scans were taken in transmittance mode in the range of 4000 to 400 cm^{-1} at a resolution of 4 cm^{-1} with the standard potassium bromide disk technique.

Experimental Design

The biochar activation experiment was repeated three times for each condition. An analysis of variance (ANOVA) model was applied to determine the significance of the experimental results *via* Fisher's protected t-test. Following the application of Fisher's protected t-test, a comparison of means test was performed by the least significant difference (LSD) method with a significance determined at the 0.05 alpha (α) level. The four treatments included KOH, H_2O_2, H_3PO_4, and heat-only. Dependent variables analyzed by the comparison of means test were activated carbon yields, total surface area, total pore volume, microporous surface area, mesoporous surface area, average pore size, and mesoporous volume.

RESULTS AND DISCUSSION

The Yield of Activated Carbon Prepared by the KOH, H_2O_2, H_3PO_4, and Heat-Only Treatments

The yields of activated carbon prepared by the KOH, H_2O_2, H_3PO_4, and heat-only treatments were calculated by Eq. 1 and are presented in Fig. 2. The activated carbon prepared by the heat-only control treatment was taken as a reference in order to evaluate samples subject to the other treatments. Figure 2 shows that the significantly highest activated carbon yield was 86.5 wt.% for the heat-only treatment. This result was expected because there was no material consumed other than the carbon during activation.

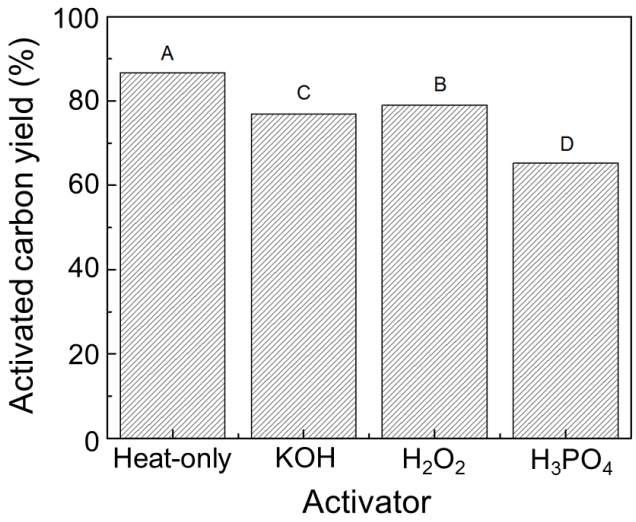

Fig. 2. The activated carbon yield after the KOH, H_2O_2, H_3PO_4, and heat-only treatments. Different letters indicate significant difference between values at an alpha level of 0.05.

The yield of the activated carbon prepared by the H_2O_2 treatment (79.3 wt.%) was significantly higher than those obtained by the KOH and H_3PO_4 treatments (76.8 and 65.4 wt.%), respectively. The mass loss for all treated specimens was due to the reaction of the chemical activators with carbon to produce the emitted gas. However, the reaction pathways and mass loss due to gas loss differed for each activator. The mechanism for the KOH treatment was the dehydration of KOH to K_2O. The K_2O reacted with CO_2 produced from the water-gas-shift reaction, producing K_2CO_3. The metallic potassium vapor was

formed above 700 °C, which eroded the framework of the carbon, leading to the rapid expansion of the carbon material, a larger surface area, and high pore volume.

BET analysis showed that the gas eroded the carbon structure and produced pores in the H_2O_2 and H_3PO_4 activated products. Figure 2 shows that mass loss due to gas discharge occurred for both activators. The possible mechanism for phosphoric acid to activate the char is that H_3PO_4 worked as an acid catalyst to promote bond cleavage reactions. This would also allow the formation of crosslinking *via* processes such as cyclization, and condensation to combine with organic species to form phosphate and polyphosphate bridges which connect and crosslink biopolymer fragments (Jagtoyen and Derbyshire 1998). Similarly, the H_2O_2 would cause acidic oxygen functional groups to form (Huff and Lee 2016) and any outgassing from the elevated temperature would exacerbate pore formations.

Adsorption-Desorption Isotherms Analysis of Activated Carbon Prepared by the KOH, H_2O_2, H_3PO_4, and Heat-Only Treatments

The characteristics of porosity and the nitrogen adsorption-desorption isotherms for activated carbon prepared by the KOH, H_2O_2, H_3PO_4, and heat-only treatments are shown in Table 1 and Fig. 3, respectively.

Table 1 summarizes the properties of the prepared activated carbons in terms of total surface area, total pore volume, microporous surface area, microporous volume, mesoporous surface area, and average pore size. There were significantly different improvements of BET properties of the activated carbon produced from the three chemical treatments compared with those of the heat-only treatment. Amaya *et al.* (2007) defined activated carbon as a product with a BET surface area greater than 200 m^2/g and total pore volume higher than 0.1 cm^3/g. The activated carbon prepared by the heat-only treatment qualified as activated carbon. KOH treatment produced the most significant improvement of pore properties. The H_3PO_4 treatment created activated carbon with a total surface area of 455.5 m^2/g. The least significant improvement using chemical methods was obtained from the H_2O_2 treatment.

Table 1. The Properties of Activated Carbon Prepared by the KOH, H_2O_2, H_3PO_4, and Heat-Only Treatments

Pyrolyzed Char Treatment	Total surface area (m^2/g)	Total pore volume (cm^3/g)	Average pore radius (nm)	Microporous surface area (m^2/g)	Mesoporous surface area (m^2/g)	Microporous volume (cm^3/g)
Heat-only	233.2 D 0%	0.138 BC 0%	1.184 B 0%	129.9 D 0%	103.3 B 0%	0.070 D 0%
KOH	1124.4 A 482%	0.723 A 524%	1.295 A 109%	932.6 A 718%	191.8 A 186%	0.485 A 693%
H_2O_2	363.0 C 156%	0.202 B 146%	1.110 C 94%	271.5 C 209%	91.6 C 89%	0.141 C 201%
H_3PO_4	455.5 B 195%	0.251 B 182%	1.102 C 93%	393.3 B 302%	62.2 D 60%	0.211 B 301%

Note: Different letters to the right of the table values indicate significant difference between values in the column using a p-value of 0.05. For comparison, the microporous volume percentage differences of chemical activator products compared to the heat-only treatment are given below the variable values.

Compared with pore properties of the activated carbon prepared by the heat-only treatment, the respective total surface areas for the KOH, H_2O_2, and H_3PO_4 treatments increased by 482%, 156%, and 195%, the total respective pore volume increased by 524%, 146%, and 182%, the respective microporous surface area increased by 718%, 209%, and 302%, and the respective microporous volume increased by 639%, 201%, and 301%.

The isothermal curves obtained from the nitrogen adsorption-desorption isotherms at -196 °C for activated carbon are shown in Fig. 3. These were compared to the standard classification of isotherms (Sing 1985). The isotherms of the activated carbon obtained by the KOH treatment are characterized as Type IV isotherms. The KOH Type IV isotherms exhibited a hysteresis loop, which is usually associated with the filling and emptying of mesopores by capillary condensation. This developed mesoporous structure produced the highest mesoporous surface area of 191.8 m^2/g, which is shown in Table 1. The isotherms shown in Fig. 3 were also analyzed in terms of adsorption-desorption hysteresis loops. The largest hysteresis loop was for the KOH treatment and indicated high mesoporosity in the activated carbon produced. In addition, this hysteresis loop suggested that the pores are slit-shaped or that the carbons were comprised of a plate-like material, and graphene layers may be between the pores (Williams and Reed 2006).

The nitrogen adsorption and desorption isotherms from activated carbon obtained from the H_3PO_4 treatment were characterized as a Type I isotherms. The type I isotherms occurred due to enhanced adsorbent-adsorbate interactions in the micropores of molecular dimensions. The narrow range of relative pressure needed to achieve the plateau gave an indication as to the limited pore size range. In addition, the isotherms were analyzed in terms of its hysteresis loop for this kind of activated carbon. The hysteresis loop was extremely small, but indicated the presence of slit shaped pores or plate-like material (Williams and Reed 2006).

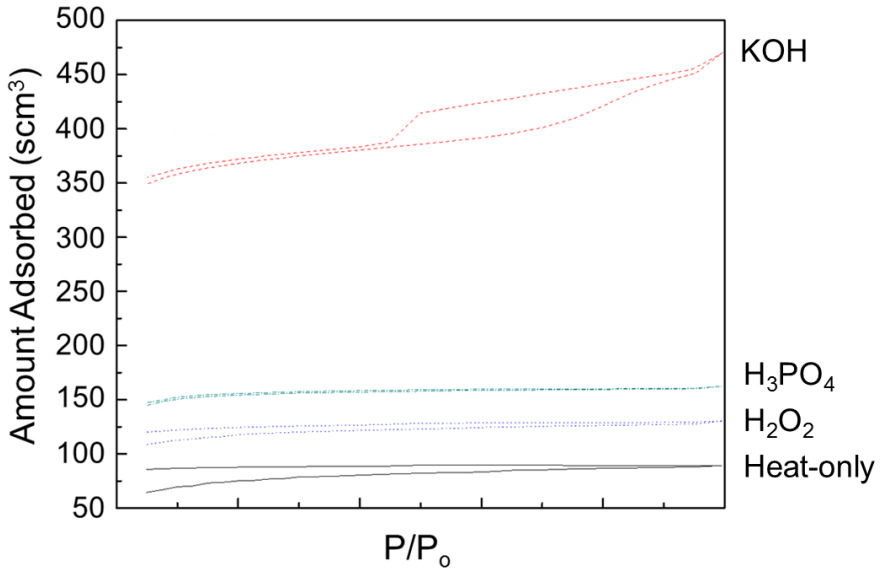

Fig. 3. Nitrogen adsorption-desorption isotherms at -196 °C for activated carbon derived from pyrolyzed biochar prepared by the KOH, H_2O_2, H_3PO_4, and heat-only treatments

The activated carbon obtained by the H_2O_2 and heat-only treatments showed nitrogen adsorption and desorption isotherms that were characterized between Type I and

Type II, which indicated a microporous structure with a less developed mesoporous structure (Greg and Sing 1985; Amaya *et al.* 2007; Yang *et al.* 2010).

Figure 4 shows the pore size distribution of activated carbon prepared by pyrolysis char treated with KOH, H_2O_2, and H_3PO_4 methods as well as the heat-only treatment. The activated carbon from the heat-only treatment shows two main pore distributions ranging from 2.5 to 3.2 nm and 3.2 to 4.8 nm, as well as a small portion of micropores, which corresponds to the BET data listed in Table 1. Both the H_2O_2 and H_3PO_4 method show one main pore distribution ranging from 2.0 to 3.2 nm. However, the main pore distribution of the products from H_2O_2 is slightly bigger than H_3PO_4 which leads to a little bigger mesoporous surface area as shown in Table 1. The KOH method formed a well-developed pore structure in the activated carbon so that it contained a large portion of micropores and mesopores which brings about a higher surface area of 1124.4 m^2/g. The KOH method also led to a mesopores with a surface area of 191.8 m^2/g.

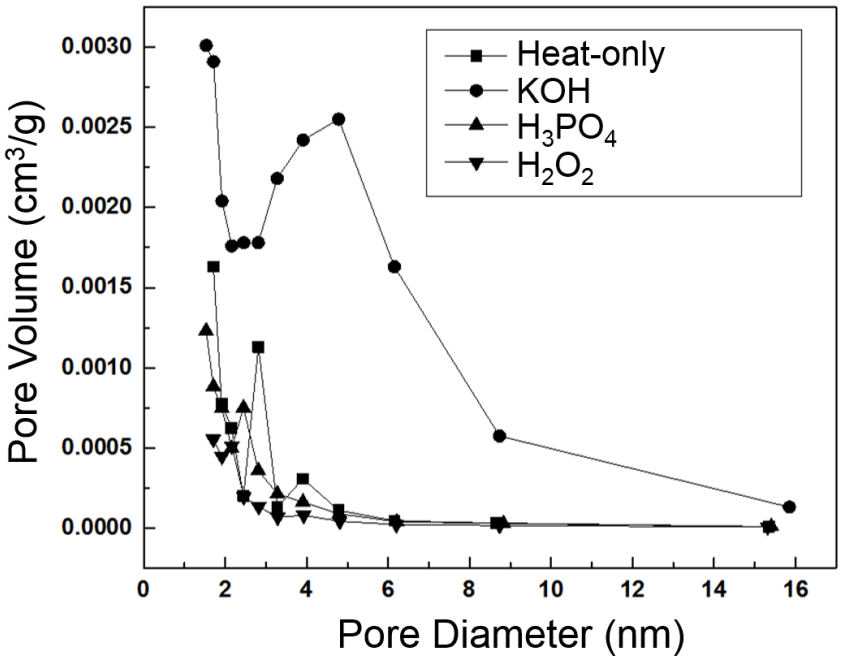

Fig. 4. Pore size distribution for activated carbon derived from pyrolyzed biochar prepared by the KOH, H_2O_2, H_3PO_4, and heat-only treatments

TEM Characterization of Activated Carbon Prepared by the KOH, H_2O_2, H_3PO_4, and Heat-Only Treatments

Figure 5 shows TEM micrographs for the activated carbons prepared by the KOH, H_2O_2, H_3PO_4, and heat-only treatments. The micrographs show that the pore structure and channels of the activated carbon prepared by the heat-only treatment were obscure. Figure 5B shows clear mesopores in the activated carbon prepared by the KOH treatment. The mesopores were mainly between 5 to 20 nm in size. This developed mesoporosity corresponded to the high mesoporous surface area given in Table 1. The mesoporosity was developed from the micropores at the expense of carbon yield, which resulted in pore widening and the development of mesoporosity. This may explain why the activated carbon yield was lower when the KOH treatment was applied. Figure 5C shows the lengths and sizes of the channels and mesopores in the activated carbon prepared by the H_2O_2 treatment.

Fig. 5D shows that the mesoporous structure and pore channels of the activated carbon prepared by the H_3PO_4 treatment were not as well developed when compared to the activated carbon treated with KOH and H_2O_2.

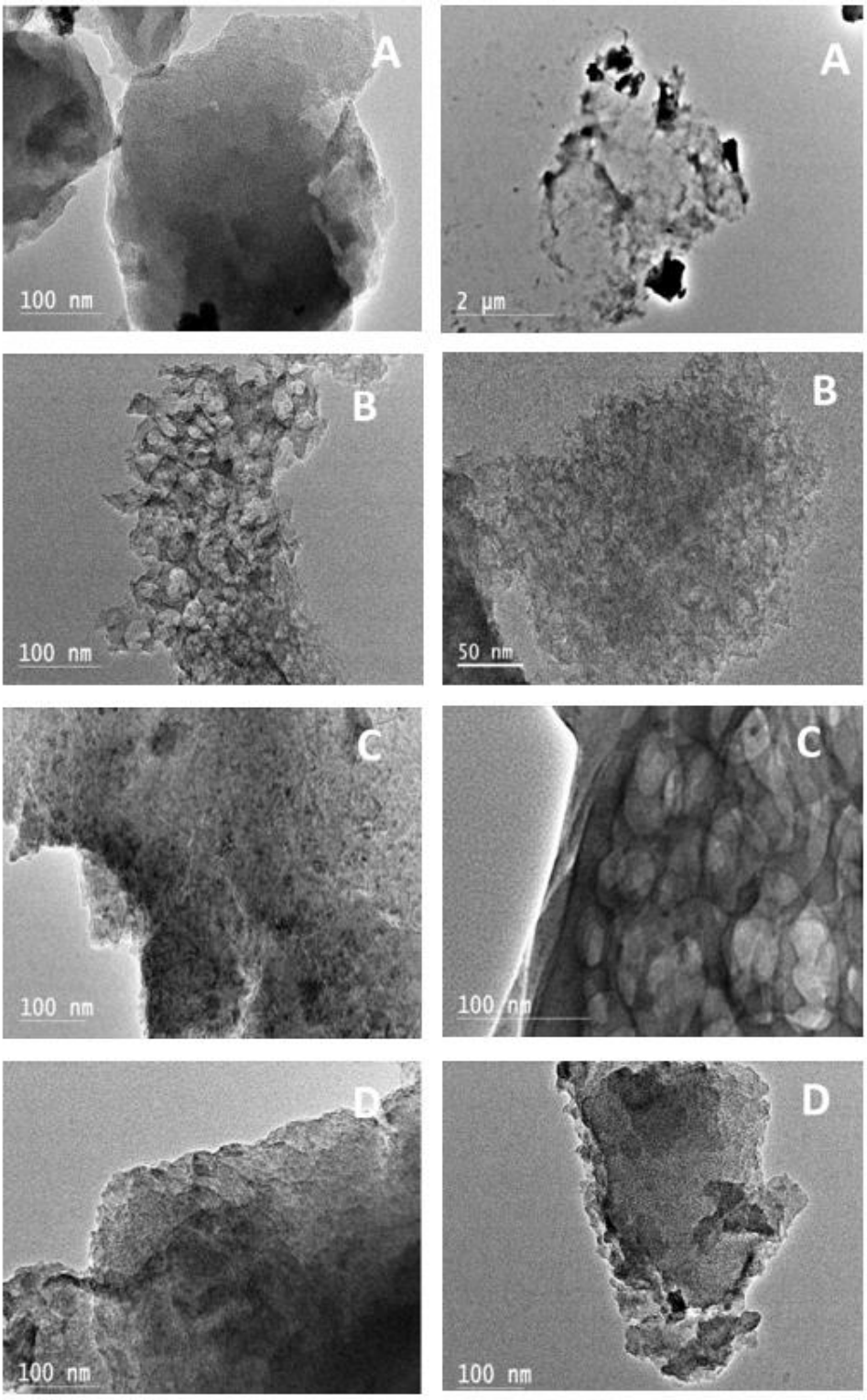

Fig. 5. TEM micrographs of activated carbon prepared by four treatments: A) Heat-Only; B) KOH; C) H_2O_2; and D) H_3PO_4

FTIR Analysis of Activated Carbon Prepared by the KOH, H_2O_2, H_3PO_4, and Heat-Only treatments

The adsorption capacity of activated carbon is determined by the specific surface area, porous distribution, structure size, and the functional groups at the surface of the activated carbon. The FTIR spectra of the four samples are shown in Fig. 6 and characterize the chemical functional groups of the activated carbon.

The spectra did not show any adsorption from 3600 to 3200 cm^{-1}, which indicated that there was no O-H stretching mode of hydroxyl groups and adsorbed water. The two spectra of the activated carbon prepared by the KOH and H_3PO_3 treatments showed a strong peak located around 1720 cm^{-1}, which was ascribed to C=O stretching vibration of ketone, aldehyde, lactones, or carboxyl groups. The strong intensity of these peaks suggested that the activated carbon prepared by the KOH and H_3PO_3 treatments contained a large number of carboxyl groups. The activated carbon prepared by the H_2O_2 treatment presented a weak peak located at 1720 cm^{-1}. This indicated that this product contained a small number of carboxyl groups. Moreover, the activated carbon from the heat-only treated pyrolyzed char did not show a peak at this wavelength. A possible explanation for this is that no oxygen molecules were added during the treatment.

Both samples prepared by the KOH and H_3PO_3 treatments showed a strong band at 1600 to 1580 cm^{-1}, which indicated the presence of an aromatic ring structure vibration (C=C). Specifically, the intensity of the peak at 1600 to 1580 cm^{-1} for the KOH treatment was slightly stronger than the one produced by the H_3PO_4 treatment, which means the former contained a higher degree of aromatic ring structure vibration (C=C). However, the activated carbon prepared by the H_2O_2 and heat-only treatments did not show any adsorption at 1600 to 1580 cm^{-1}.

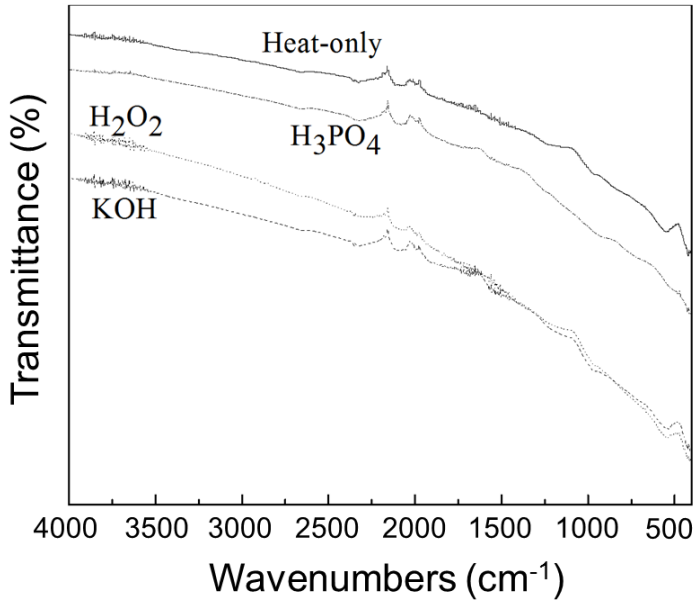

Fig. 6. FTIR spectra of activated carbons prepared by the KOH, H_2O_2, H_3PO_4, and heat-only treatments

All spectra showed a broad band between 1300 and 900 cm^{-1}, which was due to C-O stretching in acids, alcohols, phenols, esters, and ethers. The adsorption in this region for the H_3PO_4 treatment was attributed to phosphorus and phosphocarbonaceous compounds. More specifically, the peak at 1220 to 1180 cm^{-1} may have been due to the

stretching mode of hydrogen-bonded P=O, O-C stretching vibration in P-O-C (aromatic) linkage, and P=OOH. The peak at 1080 to 1070 cm^{-1} may have been due to ionized linkage P^{+}-O^{-} in acid phosphate ester and a symmetrical vibration in a chain of P-O-P (polyphosphate) (Puziy *et al.* 2002; Guo and Rockstraw 2007).

TGA Analysis of Activated Carbon Prepared by the KOH, H_2O_2, H_3PO_4, and Heat-Only Treatments

Figure 7 presents the weight-loss curves corresponding to the increasing temperature of activated carbons prepared by the KOH, H_2O_2, H_3PO_4, and heat-only treatments. The TGA curve of the activated carbon prepared by the H_2O_2 treatment was similar to the activated carbon TGA curve prepared by the heat-only treatment. Both treatments had a relative mass loss of 16 wt.% between 30 to 1000 °C and a relative mass loss of approximately 9 wt.% between 30 and 100 °C, which corresponded to the removal of moisture or gas adsorbed on the activated carbon (Sricharoenchaikul *et al.* 2007). The activated carbon prepared with the KOH treatment showed a relative mass loss of 21 wt.%, which was 31% higher than the H_2O_2 and heat-only treatments. The 16 wt.% relative mass loss between 30 to 100 °C most likely occurred because the high surface areas of the activated carbon adsorbed more moisture or gas when exposed to the air. The activated carbon prepared by the H_3PO_4 treatment also had similar results. The first 18 wt.% mass loss was observed below 100 °C and was attributed to the removal of moisture (Sricharoenchaikul *et al.* 2007) or gas adsorbed on the surface of the activated carbon. The second weight loss for the H_3PO_4 treatment began at 800 °C, and the rate of the weight loss was much more noticeable at this point than for the other treatments. One possible explanation is that the structure of activated carbon with the phosphorous species was decomposing at this temperature.

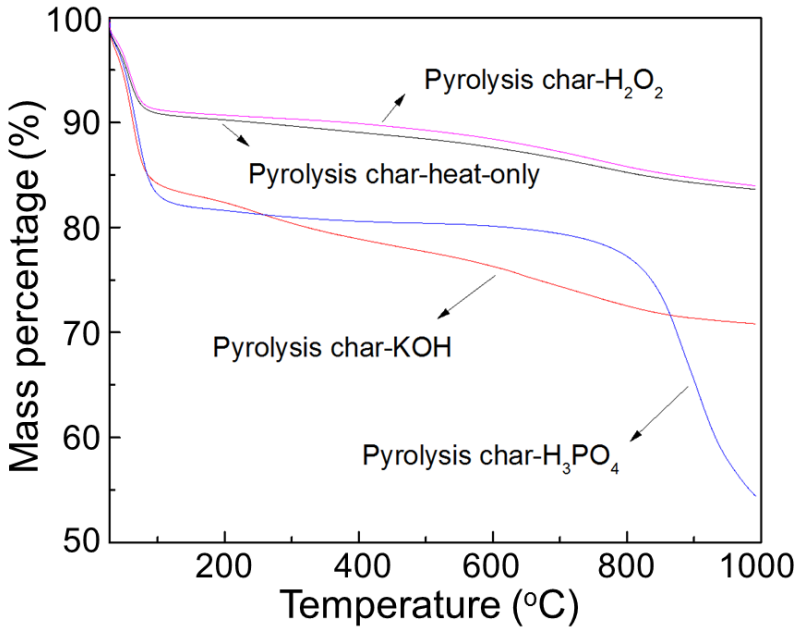

Fig. 7. TGA curves of activated carbon prepared by the KOH, H_2O_2, H_3PO_4, and heat-only treatments

CONCLUSIONS

1. Activated carbon prepared from the pyrolysis of pinewood using KOH, H_2O_2, and H_3PO_4 treatments led to better pore properties than using the heat-only treatment. The yield of activated carbon ranged from 65 to 85 wt.%, depending on the activation method.
2. The surface area and total pore volume of the activated carbon obtained by H_2O_2 and H_3PO_4 were higher than that of activated carbon obtained from the heat-only treatment, but they were considerably lower than the KOH treatment. Activated carbon prepared using the KOH treatment had the significantly highest BET surface area of 1124.4 m^2/g and a total pore volume of 0.73 cm^3/g.
3. TEM micrographs showed that the activated carbon prepared by the KOH and H_2O_2 treatments exhibited a more developed and clear mesoporosity than the heat-only and H_3PO_4 treatments.
4. TGA curves indicated that activated carbon prepared by KOH had a relative mass loss of 29 wt.%. The activated carbon prepared by the heat-only and H_2O_2 treatments had a relative mass loss of 16 wt.%. The H_3PO_4 treatment had a relative mass loss of 45 wt.%.

ACKNOWLEDGEMENTS

This material is based upon work that is supported by the National Institute of Food and Agriculture, U.S. Department of Agriculture, and McIntire Stennis under 1008126. The authors wish to acknowledge the support of the U.S. Department of Agriculture (USDA), Research, Education, and Economics (REE), Agriculture Research Service (ARS), Administrative and Financial Management (AFM), Financial Management and Accounting Division (FMAD), and Grants and Agreements Management Branch (GAMB), under Agreement No. 5B-0202-4-001. This report was prepared as an account of work sponsored by an agency of the United States Government. Neither the United States Government nor any agency thereof, nor any of their employees, makes any warranty, express or implied, or assumes any legal liability or responsibility for the accuracy, completeness, or usefulness of any information, apparatus, product, or process disclosed, or represents that its use would not infringe privately owned rights. Reference herein to any specific commercial product, process, or service by trade name, trademark, manufacturer, or otherwise does not necessarily constitute or imply its endorsement, recommendation, or favoring by the United States Government or any agency thereof. The views and opinions of authors expressed herein do not necessarily state or reflect those of the United States Government or any agency thereof. Any opinions, findings, conclusions, or recommendations expressed in this publication are those of the author(s) and do not necessarily reflect the views of the U.S. Department of Agriculture. This research is based upon work funded through MAFES/FWRC Director's Fellowship Awards at Mississippi State University (MSU). The authors would like to thank I-Wei Chu of the Institute for Imaging & Analytical Technologies and Mr. Brian Mitchell of the Department of Sustainable Bioproducts, MSU, for their analysis assistance and production of pinewood char for this work. This material is held at the Mississippi State University Forest and Wildlife Research Center under the manuscript designation SB845.

REFERENCES CITED

Amaya, A., Medero, N., Tancredi, N., Silva, H., and Deiana, C. (2007). "Activated carbon briquettes from biomass materials," *Bioresource Technol.* 98(8), 1635-1641. DOI: 10.1016/j.biortech.2006.05.049

Cunliffe, A. M., and Williams, P. T. (1999). "Influence of process conditions on the rate of activation of chars derived from pyrolysis of used tires," *Energ. Fuels* 13(1), 166-175. DOI: 10.1021/ef9801524

Duman, G., Onal, Y., Okutucu, C., Onenc, S., and Yanik, J. (2009). "Production of activated carbon from pine cone and evaluation of its physical, chemical, and adsorption properties," *Energ. Fuels* 23(4), 2197-2204. DOI: 10.1021/ef800510m

Gregg, S., and Sing, K. (1982). *Adsorption, Surface Area, and Porosity*, Academic Press, London, UK.

Guo, Y., and Rockstraw, D. A. (2007). "Physicochemical properties of carbons prepared from pecan shell by phosphoric acid activation," *Bioresource Technol.* 98(8), 1513-1521. DOI: 10.1016/j.biortech.2006.06.027

Huff, M. D., and Lee, J. W. (2016). "Biochar-surface oxygenation with hydrogen peroxide," *J. Envir. Management.* 165, 17-21. DOI: 10.1016/j.jenvman.2015.08.046

Ingram, L., Mohan, D., Bricka, M., Steele, P., Strobel, D., Crocker, D., Mitchell, B., Mohammad, J., Cantrell, K., and Pittman Jr, C. U. (2007). "Pyrolysis of wood and bark in an auger reactor: Physical properties and chemical analysis of the produced bio-oils," *Energ. Fuels* 22(1), 614-625. DOI: 10.1021/ef700335k

Jagtoyen, M., and Derbyshire, F. (1988). "Activated carbons from yellow poplar and white oak by H_3PO_4 activation," *Carbon*, 36 (7–8), 1085-1097. DOI: 10.1016/S0008-6223(98)00082-7

Khummongkol, D., Charoenkool, A., and Pongkum, N. (1992). "Experimental optimization of activated carbon synthesis by the simplex search method," *Appl. Energ.* 41(4), 243-249. DOI: 10.1016/0306-2619(92)90005-V

Kołodyńska, D., Wnętrzak, R., Leahy, J. J., Hayes, M. H. B., Kwapiński, W., and Hubicki, Z. (2012). "Kinetic and adsorptive characterization of biochar in metal ions removal," *Chem. Eng. J.* 197, 295-305. DOI: 10.1016/j.cej.2012.05.025

Luo, Y., Guda, V. K., Hasan, E. B., Steele, P. H., Mitchell, B., and Yu, F. (2016a). "Hydrodeoxygenation of oxidized distilled bio-oil for the production of gasoline fuel type," *Energ. Convers. Manage.* 112, 319-327. DOI: 10.1016/j.enconman.2015.12.047

Luo, Y., Hassan, E. B. M., Guda, V., Wijayapala, R., and Steele, P. H. (2016b). "Upgrading of syngas hydrotreated fractionated oxidized bio-oil to transportation grade hydrocarbons," *Energ. Convers. Manage.* 115, 159-166. DOI: 10.1016/j.enconman.2016.02.051

Luo, Yan, Guda, V. K, Steele, P. H., and Wan, H (2016c). "Hydrodeoxygenation of oxidized and hydrotreated bio-oils to hydrocarbons in fixed-bed continuous reactor," BioResources, 11 (2), 4415-4431.

Macías-García, A., Garrído-Calero, J. R., Fernández González, M. C., and Gómez-Serrano, V. (2007). "Preparation and characterization of activated carbons by activation with H_3PO_4," *J. Adv. Mater.* 39(1), 28-32.

Oasmaa, A., Solantausta, Y., Arpiainen, V., Kuoppala, E., and Sipilä, K. (2009). "Fast pyrolysis bio-oils from wood and agricultural residues," *Energ. Fuels* 24(2), 1380-1388. DOI: 10.1021/ef901107f

Puziy, A. M., Poddubnaya, O. I., Martínez-Alonso, A., Suárez-García, F., and Tascón, J. M. D. (2002). "Synthetic carbons activated with phosphoric acid: I. Surface chemistry and ion binding properties," *Carbon* 40(9), 1493-1505. DOI: 10.1016/S0008-6223(01)00317-7

Rios, R. B., Silva, F. W. M., Torres, A. E. B., Azevedo, D. C. S., and Cavalcante Jr, C. L. (2009). "Adsorption of methane in activated carbons obtained from coconut shells using H_3PO_4 chemical activation," *Adsorption* 15(3), 271-277. DOI: 10.1007/s10450-009-9174-9

Rodríguez-Reinoso, F., and Molina-Sabio, M. (1992). "Activated carbons from lignocellulosic materials by chemical and/or physical activation: An overview," *Carbon* 30(7), 1111-1118. DOI: 10.1016/0008-6223(92)90143-K

Sing, K. S. W. (1985). "Reporting physisorption data for gas/solid systems with special reference to the determination of surface area and porosity (Recommendations 1984)," *Pure Appl. Chem.* 57(4), 603-619. DOI: 10.1351/pac198557040603

Sricharoenchaikul, V., Pechyen, C., Aht-ong, D., and Atong, D. (2007). "Preparation and characterization of activated carbon from the pyrolysis of physic nut (*Jatropha curcas* L.) waste," *Energ. Fuels* 22(1), 31-37. DOI: 10.1021/ef700285u

Tay, T., Ucar, S., and Karagöz, S. (2009). "Preparation and characterization of activated carbon from waste biomass," *J. Hazard. Mater.* 165(1–3), 481-485. DOI: 10.1016/j.jhazmat.2008.10.011

Williams, P. T., and Reed, A. R. (2006). "Development of activated carbon pore structure *via* physical and chemical activation of biomass fibre waste," *Biomass Bioenerg.* 30(2), 144-152. DOI: 10.1016/j.biombioe.2005.11.006

Woolf, D., Amonette, J. E., Street-Perrott, F. A., Lehmann, J., and Joseph, S. (2010). "Sustainable biochar to mitigate global climate change," *Nature Communications* 1(56). DOI: 10.1038/ncomms1053

Yang, K., Peng, J., Srinivasakannan, C., Zhang, L., Xia, H., and Duan, X. (2010). "Preparation of high surface area activated carbon from coconut shells using microwave heating," *Bioresource Technol.* 101(15), 6163-6169. DOI: 10.1016/j.biortech.2010.03.001

Zabaniotou, A., Stavropoulos, G., and Skoulou, V. (2008). "Activated carbon from olive kernels in a two-stage process: Industrial improvement," *Bioresource Technol.* 99(2), 320-326. DOI: 10.1016/j.biortech.2006.12.020

Article submitted: July 27, 2016; Peer review completed: October 2, 2016; Revised version received and accepted: October 21, 2016; Published: October 26, 2016.
DOI: 10.15376/biores.11.4.10433-10447